Ca^{2+} and frequency dependence of exocytosis in isolated somata of magnocellular supraoptic neurones of the rat hypothalamus

Brandi L. Soldo[1], David R. Giovannucci[2], Edward L. Stuenkel[1] and Hylan C. Moises[1]

[1]*Department of Molecular and Integrative Physiology, University of Michigan Medical School, Ann Arbor, MI 48109-0622, USA*
[2]*Department of Anatomy and Neurobiology, Medical College of Ohio, 3036 Arlington Avenue, Toledo, OH 43614, USA*

In addition to action potential-evoked exocytotic release at neurohypophysial nerve terminals, the neurohormones arginine vasopressin (aVP) and oxytocin (OT) undergo Ca^{2+}-dependent somatodendritic release within the supraoptic and paraventricular hypothalamic nuclei. However, the cellular and molecular mechanisms that underlie this release have not been elucidated. In the present study, the whole-cell patch-clamp technique was utilized in combination with high-time-resolved measurements of membrane capacitance (C_m) and microfluorometric measurements of cytosolic free Ca^{2+} concentration ($[Ca^{2+}]_i$) to examine the Ca^{2+} and stimulus dependence of exocytosis in the somata of magnocellular neurosecretory cells (MNCs) isolated from rat supraoptic nucleus (SON). Single depolarizing steps ($\geq$20 ms) that evoked high-voltage-activated (HVA) Ca^{2+} currents (I_{Ca}) and elevations in intracellular Ca^{2+} concentration were accompanied by an increase in C_m in a majority (40/47) of SON neurones. The C_m responses were composed of an initial Ca^{2+}-independent, transient component and a subsequent, sustained phase of increased C_m (termed ΔC_m) mediated by an influx of Ca^{2+}, and increased with corresponding prolongation of depolarizing step durations (20–200 ms). From this relationship we estimated the rate of vesicular release to be 1533 vesicles s^{-1}. Delivery of neurone-derived action potential waveforms (APWs) as stimulus templates elicited I_{Ca} and also induced a ΔC_m, provided APWs were applied in trains of greater than 13 Hz. A train of APWs modelled after the bursting pattern recorded from an OT-containing neurone during the milk ejection reflex was effective in supporting an exocytotic ΔC_m in isolated MNCs, indicating that the somata of SON neurones respond to physiological patterns of neuronal activity with Ca^{2+}-dependent exocytotic activity.

(Received 11 July 2003; accepted after revision 20 November 2003; first published online 28 November 2003)
Corresponding author D. Giovannucci: Department of Anatomy and Neurobiology, Medical College of Ohio, 3036 Arlington Avenue, Toledo, OH 43614, USA. Email: dgiovannucci@mco.edu

The process of Ca^{2+}-dependent exocytotic fusion underlies the release of neurotransmitters for fast synaptic transmission and the secretion of neuropeptide hormones from presynaptic axon terminals. However, in addition to presynaptic sites of exocytosis, recent evidence indicates a strong likelihood for significant extrasynaptic vesicular release from somatodendritic regions of central and peripheral neurones, including those of the substantia nigra (Cheramy *et al.* 1981; Jaffe *et al.* 1998), dorsal root ganglia (Huang & Neher, 1996), and hypothalamic SON (Mason *et al.* 1984; Moos *et al.* 1984; Di Scala-Guenot *et al.* 1987). The voltage and ionic dependence of this activity points to the involvement of Ca^{2+}-dependent secretory mechanisms similar to those described for more conventional presynaptic sites of activity-dependent vesicular exocytosis (Giovannucci & Stuenkel, 1997; Soldo *et al.* 1998; De Kock *et al.* 2003). Thus, it has been suggested that somatodendritic release may function to regulate the behaviour of specific classes of neurones at the level of the cell body in an autocrine or paracrine fashion via extrasynaptic mechanisms.

Magnocellular neurosecretory cells (MNCs) of the SON are responsible for the synthesis and vesicular packaging of the neurohormones aVP and OT, which are then

B. L. Soldo and D. R. Giovannucci contributed equally to this work.

DOI: 10.1113/jphysiol.2003.051136

released into the bloodstream from their neurosecretory terminals within the neurohypophysis. In addition, results from push–pull perfusion or microdialysis experiments conducted *in vivo* and radioimmunological detection of peptide release from SON tissue explants have demonstrated that depolarization of MNCs, whether induced experimentally or by physiological stimuli such as parturition and suckling, elicits significant intranuclear release of OT *within* the SON (Mason *et al.* 1984; Di Scala-Guenot *et al.* 1987; Moos *et al.* 1989; Neumann *et al.* 1993). Interestingly, this stimulated intranuclear secretion appeared to be decoupled from systemic release of the peptide, in that it continued after abatement of release of the neurohormone from the neurosecretory endings of the SON neurones (Neumann *et al.* 1993). It was further shown that exogenous application of OT to isolated SON *in vitro* induced Ca^{2+}-dependent release of OT (Moos *et al.* 1984), and that this action correlated with the ability of OT to enhance the burst firing of OT-containing SON neurones (Lambert *et al.* 1993). On the basis of these data it has been posited that the functional role of intranuclear release of OT is to facilitate its continued secretion by providing positive feedback via postsynaptic receptors within the hypothalamic nuclei. By contrast, the activity of SON neurones was found to be reduced when OT acted at presynaptic receptors located on excitatory afferent inputs to the nucleus (Kombian *et al.* 1997). While the primary origin for the intranuclear release of OT remains unclear, the finding in anatomical studies that the rat SON contains few recurrent axonal collaterals (Mason *et al.* 1984) favours a major contribution from the dendrites and possibly somata of MNCs. Consistent with a somatodendritic origin of this intranuclear release are ultrastructural data that demonstrate the presence of large, dense-core secretory granules at somatic and dendritic sites in OT- and aVP-containing SON neurones and their clustering following high-potassium-induced depolarization (Pow & Morris, 1989; Wang *et al.* 1995). In addition, stimulus-induced somatic release is abolished following treatment of OT neurones with tetanus toxin, implicating exocytotic fusion in this process (De Kock *et al.* 2003).

A powerful and now widely adopted approach for monitoring secretory events in both endocrine cells and isolated nerve endings is to measure time-resolved changes in C_m (Neher & Marty, 1982; Joshi & Fernandez, 1988; Lindau & Neher, 1988). Changes in C_m (referred to here as ΔC_m) that are elicited in response to depolarization reflect changes in cell surface area due to the addition (exocytosis) or retrieval (endocytosis) of vesicular membrane and provide an 'on line' measure of secretory activity at the single cell level. Only recently has this method been applied to investigate the exocytotic activity of MNC somata (De Kock *et al.* 2003). In the present study, we monitored ΔC_m in combination with whole-cell patch recording of I_{Ca} and fura-2 microfluorometry to determine the characteristics of Ca^{2+}-dependent vesicular release from the somata of supraoptic MNCs. Additionally, we sought to determine whether depolarization of neurones using physiologically relevant stimulus templates modelled on neurone-derived action potentials could activate exocytosis. We demonstrate that membrane depolarizations that elicited robust I_{Ca} and Ca^{2+} influx evoked substantial ΔC_m responses. However, the exocytotic fusion of non-secretory organelles can be induced by high, non-physiological elevations in cytosolic Ca^{2+} (for example, that induced by photolysis of caged Ca^{2+} or intense stimulation by repetitive step depolarizations). Thus in addition in the current study we used physiologically relevant action potential based stimulation protocols to drive the fusion of secretory granules. Application of trains of action potential waveforms activated ΔC_m in the somata of MNC in a frequency-dependent manner. These data indicate that the somata of SON neurones contain functional exocytotic machinery to perform Ca^{2+}-dependent secretion.

Methods

Neurone preparation

Acutely dissociated neurones of the hypothalamic SON were prepared from postnatal 17- to 25-day-old Sprague–Dawley rats as previously described (Soldo & Moises, 1998). Briefly, 400–500 μm slices containing the basal hypothalamic nucleus were collected. Segments of tissue containing the SON were dissected from regions adjacent to either side of the optic chiasm. The tissue fragments were enzymatically treated at 37°C with trypsin (Type I, 1.25 mg ml^{-1}; Sigma, St Louis, MO, USA) and mechanically dissociated using several passages through a fire-polished Pasteur pipette. Dissociated neurones were plated onto poly-L-lysine-coated 35 mm culture dishes. Growth medium containing nerve growth factor was added approximately 1 h after plating. Neurones that had well-rounded cell bodies (14–38 μm) with no or only a few short extending processes were studied from 3 h to 1 day after plating. In a previous report, we had identified neurones of similar morphology as aVP- and OT-containing magnocellular SON neurones (Soldo & Moises, 1998).

All animals were handled in accordance with University of Michigan Institutional Animal Care Committee and

NIH guidelines. Animals were deeply anaesthetized by CO_2 gas and decapitated.

Electrophysiological recording of I_{Ca} and C_m

Voltage- and current-clamp recordings were obtained using the whole-cell variation of the patch clamp technique (Hamill *et al.* 1981). Patch electrodes, prepared from glass microhaematocrit capillary tubes (i.d. = 1.1–1.2 mm, o.d. = 1.3–1.4 mm; Fisher Scientific, Pittsburgh, PA, USA) and having resistances of 3–5 MΩ, were coated with Sylgard elastomer (Dow Corning, Midland, MI, USA). The voltage-clamp patch electrodes were filled with an internal recording solution of composition (mM): 102 caesium acetate, 11 CsCl, 1 $MgCl_2$, 5 4-aminopyridine, 40 Hepes, 0.250 EGTA, 4 ATP, 0.1 GTP (pH 7.25–7.3; 290–300 mosmol $(kg\ H_2O)^{-1}$). In some experiments, the spatially averaged intrasomatic $[Ca^{2+}]_i$ was determined by replacing 0.15 mM EGTA of the intracellular recording solution with the same concentration of the cell-impermeant Ca^{2+}-sensitive fluorescent indicator fura-2 pentapotassium salt (Molecular Probes, Eugene, OR, USA). $[Ca^{2+}]_i$ was monitored by dual-wavelength microspectrofluorometry in a manner that has been previously detailed (Giovannucci & Stuenkel, 1997). For current-clamp recordings of somatic action potentials, electrodes were filled with the following internal solution (mM): 130 potassium gluconate, 2 $MgCl_2$, 10 Hepes, 1 EGTA, 0.5 $CaCl_2$, 2 ATP, 0.1 GTP. Plated neurones were viewed through an inverted microscope and continuously superfused with a physiological saline of composition (mM): 140 NaCl, 1.2 $MgCl_2$, 2.4 $CaCl_2$, 10 Hepes, 11 glucose. For the recording of I_{Ca}, 140 mM NaCl in the extracellular solution was replaced with 100 mM tetraethylammonium chloride (TEA-Cl), 67 mM choline-Cl and 3.5 mM KCl. Both solutions were adjusted to pH 7.2–7.3 and 300–310 mosmol $(kg\ H_2O)^{-1}$. Current records were digitally corrected for leak currents by using an on-line *P*/4 subtraction protocol.

All recordings were made at room temperature using either an Axopatch 200A amplifier (Axon Instruments, Inc., Union City, CA, USA) or EPC9 amplifier (Heka, Lambrecht, Germany). Whole-cell capacitance (15–30 pF) and series resistance (6–10 MΩ) were corrected using compensation circuitry on the patch clamp amplifier. Series resistance compensation of 75–85% was typically obtained without inducing oscillations. High-resolution C_m measurements were used to monitor changes in membrane surface area (exocytotic activity) in response to large step depolarizations. The use of the whole-cell patch-clamp technique allows for the measurement of small, time-resolvable changes in C_m (ΔC_m) by using a modified phase-tracking method (Joshi & Fernandez, 1988). ΔC_m of isolated SON neurones was measured by monitoring the current response to a 30 mV r.m.s. sine wave at 1201 Hz applied to a holding potential of −90 mV. The current output of the voltage-clamp was monitored at two orthogonal phase angles, and the correct phase angle determined using a software-based phase-sensitive detector (Pulse Control 4.5, Richard J. Bookman, University of Miami, FL, USA). A 19.1 kHz sampling rate (16 samples per sinusoidal period) was used to compute one C_m point each 13.31 ms. Calibration pulses of 100 fF and 500 kΩ were generated at the beginning of each trace by the whole cell compensation circuit and by dithering of the phase-tracking resistor, respectively.

Depolarizing voltage step commands of varying duration (5–200 ms) were applied from a holding potential (V_h) of −90 mV to generate inward I_{Ca} and to evoke ΔC_m for each neurone tested. In later experiments, an action potential was recorded under current clamp from a representative SON neurone and reintroduced as the stimulus waveform during voltage clamp recording. These action potential waveforms were applied at various frequencies to activate I_{Ca} and C_m responses. Bath solutions were applied by local superfusion of the individual neurone under study using a modified U-tube delivery system as previously described (Soldo & Moises, 1998). All data were analysed using an unpaired Student's *t* test, unless otherwise indicated, and expressed as means ± S.E.M. in the text.

Results

Features of depolarization-induced C_m responses in isolated SON neurones

To examine for depolarization-evoked exocytosis in isolated SON neurones, measurements of I_{Ca}, the associated changes in capacitance (ΔC_m) and (in selected experiments) intracellular Ca^{2+} levels ($[Ca^{2+}]_i$) were performed under whole-cell patch clamp and with ionic conditions that isolated I_{Ca}. Baseline C_m was monitored for a period of 1 s after which the neurone was depolarized by a single 200 ms voltage step to +10 mV from a V_h of −90 mV. This voltage clamp protocol elicited maximum inward I_{Ca} responses in virtually all neurones examined under standard recording conditions and was therefore uniformly employed (unless otherwise indicated) to assess their capacity for Ca^{2+}-dependent exocytosis. The I_{Ca} responses of SON consisted of both rapidly inactivating and more sustained components, as revealed by inspection

of the traces from three neurones depicted in Fig. 1*A* (lower traces). These currents have been previously characterized in detail in terms of their biophysical and pharmacological properties (Fisher & Bourque, 1995; Foehring & Armstrong, 1996; Soldo & Moises, 1998).

In response to a single depolarizing step to +10 mV, a large increase in C_m above baseline was detected in nearly all neurones examined (in 40/47 neurones; Fig. 1*A* upper traces). The depolarization-evoked C_m responses could be resolved into several kinetically distinct phases, beginning with an initial, rapidly activating transient component observed within 5–10 ms after termination of the voltage pulse, which we will refer to here as ΔC_t. This response was followed by a slower and more prolonged phase of increased C_m that differed from neurone to neurone in its peak amplitude, duration and rate of decay (compare cells 1, 2 and 3, Fig. 1*A*). When isolated from ΔC_t (see below), the latter response was represented in 37/40 neurones by an initial jump in C_m followed by a slower return of C_m to the resting level over a period of a few seconds (Fig. 1*A*, cell 1). In the three remaining neurones, the C_m responses were kinetically more complex and included a slowly increasing phase that developed with variable latencies after the initial jump in C_m (Fig. 1*A*, cell 2).

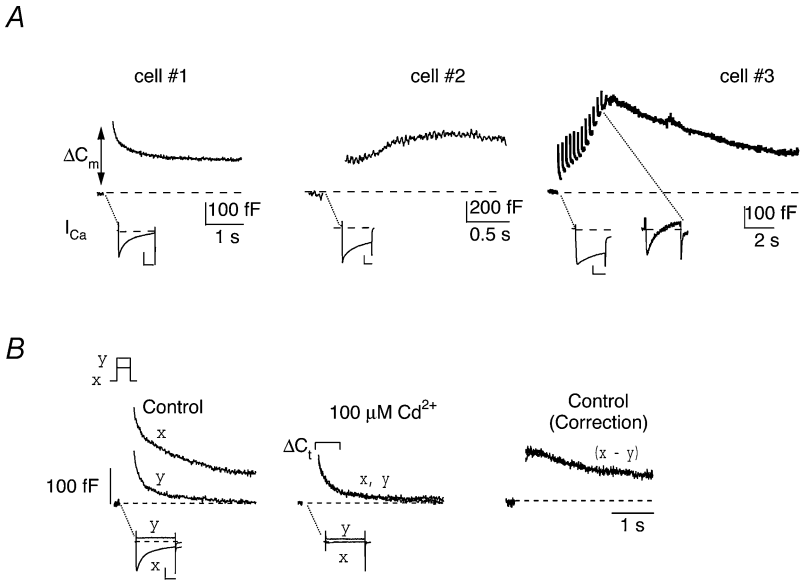

Figure 1. Depolarization-induced C_m responses recorded from MNC somata
A, representative traces of C_m (top) and corresponding I_{Ca} (bottom) responses recorded from three different neurones. Step depolarization to +10 m*V* for 200 ms from $V_h = -90$ m*V* evoked high-voltage-activated inward I_{Ca} in each neurone that differed in peak amplitude and rate of inactivation. In cells labelled 1 and 2, a jump-like increase in C_m was detected following delivery of a single depolarizing step. These C_m responses were of long duration, typically lasting several seconds and in the case of one neurone, included a slowly developing second phase of gradually increasing C_m (cell 2). In the third neurone, repetitive depolarization to +10 mV with a train of 12 pulses (50 ms in duration with 200 ms interpulse interval) evoked stepwise increases in C_m that summed to form a robust and prolonged phase of increased C_m, which decayed slowly back toward baseline over many seconds (cell 3). Note that significant Ca^{2+}-dependent inactivation of I_{Ca} occurred upon delivery of each successive pulse within the train (currents evoked by the initial and last test pulse are shown for comparison, lower traces). *B*, records from another MNC illustrate I_{Ca} (lower) and C_m responses (upper) evoked by depolarizing steps to +10 mV (trace *x*) or +70 mV (trace *y*) from $V_h = -90$ mV in control media (left panel) and in the presence of the Ca^{2+} channel blocker, Cd^{2+} (100 μM) (middle panel). Stepping to +10 mV in control (left panel) evoked substantial inward I_{Ca} (trace *x*), accompanied by a large increase in C_m (trace *x*), consisting of a transient initial response and subsequent sustained phase with slower decay. By contrast, stepping to +70 m*V* in control (trace *y,* left panel) or to either test potential in the presence of Cd^{2+} (traces *x* and *y*, middle panel) evoked negligible I_{Ca}. Note that under these conditions where Ca^{2+} influx was negligible, only the transient component of the C_m increase was detected following depolarization to +10 mV (trace*x* in Cd^{2+}) or +70 mV (trace*y* in control and Cd^{2+}). To control for contamination of depolarization-evoked changes in C_m by this transient component (termed ΔC_t in the text), *control* ΔC_m responses were corrected as shown (*x* – *y* trace, right panel) by subtracting the Ca^{2+}-independent ΔC_t evoked by depolarization to +70 m*V* (trace *y*) from the total ΔC_m evoked by a step to +10 mV (trace*x*). Verticalscale bars are 0.5 nA and 1 nA for current traces in *A* and *B*, respectively, and the time scale is 50 ms in all cases.

C_m responses of this type were more reliably observed when neurones were stimulated repetitively with trains of step depolarizations (8–12 voltage pulses; Fig. 1*A*, cell 3). Based on their similarity to exocytotic ΔC_m responses described in MNC nerve terminals (Lim *et al.* 1990; Hsu & Jackson, 1996; Giovannucci & Stuenkel, 1997), we interpret the initial jump and latent increases in C_m to reflect increases in membrane surface area that occur in response to depolarization-induced influx of Ca^{2+} and activation of Ca^{2+}-dependent vesicular fusion. Conversely, the subsequent decay of ΔC_m back to baseline has been shown to correspond to the net retrieval of vesicular membrane as the rate of endocytosis eventually exceeds that of the exocytotic response.

Correction of ΔC_m for a Ca^{2+}-independent C_m signal

The component referred to here as ΔC_t closely resembled a transient, Ca^{2+}-independent C_m response to membrane depolarization that has been observed both in the isolated nerve endings of SON neurones (Giovannucci & Stuenkel, 1997) and in bovine adrenal chromaffin cells (Horrigan & Bookman, 1994). These transient C_m signals were found to be unrelated to Ca^{2+}-dependent exocytosis, but rather were attributed to a redistribution of voltage-sensitive gating charges within the membrane (Bezanilla *et al.* 1982; Horrigan & Bookman, 1994; Debus *et al.* 1995). The ΔC_t detected in SON neurones was reliably evoked under conditions of Ca^{2+} channel blockade (100 μM Cd^{2+}), as well as following depolarizations to potentials close to the estimated value of E_{Ca} (+70 mV under our recording conditions; Fig. 1*B*). Similar to that previously shown for nerve endings, the ΔC_t amplitude was found to follow a Boltzmann-type relationship and saturated at steps above 0 mV (Giovannucci & Stuenkel, 1997). These results indicate that ΔC_t was dissociated from voltage-dependent influx of Ca^{2+} and thus does not reflect Ca^{2+}-dependent exo-endocytotic activity. As the presence of ΔC_t interferes with measurement of the Ca^{2+}-dependent C_m response, a correction was performed on all C_m measurements by doing a point by point subtraction of the ΔC_t elicited by a +70 mV voltage step from the entire ΔC_m response obtained upon depolarization to a test potential (routinely +10 mV) that elicited maximum inward I_{Ca} (Fig. 1*B*, correction trace). Henceforth, the term ΔC_m will be used for the corrected step depolarization-evoked C_m responses recorded in MNC somata.

Properties of ΔC_m in SON neurones

The amplitude of the depolarization-evoked ΔC_m varied significantly between neurones (cf. traces from 3 neurones in Fig. 1*A*), despite the fact that the magnitude and duration of the depolarizing test pulse were adjusted to produce maximal inward I_{Ca} responses. On the other hand, successive ΔC_m that were evoked in a given neurone remained relatively constant for approximately 20 min following patch rupture, after which rundown in the C_m response was common in all SON neurones tested. The variability in response among neurones, as well as the time-related changes in ΔC_m can be attributed in part to differences in the magnitude of Ca^{2+} influx and secretory capacity of individual neurones. Presumably these differences correspond to the surface area of the respective somata (94–452 μm^2), the number and subtype complement of Ca^{2+} channels, and/or in the respective number of proximal dendrites or axon stump length. The peak ΔC_m recorded in 10 neurones in response to a single 200 ms depolarizing step that evoked maximal I_{Ca} ranged between 128 and 432 fF (mean ± S.E.M.; 248 ± 35 fF). These values correspond to the fusion of approximately 345 vesicles, assuming a dense-core vesicle diameter of 160 nm (Pow & Morris, 1989) and specific membrane capacitance of 9 fF μm^{-2} (Gentet *et al.* 2000). Nevertheless, this value should be considered a low estimate since exocytosis was likely to be initiated before the end of the voltage pulse. Moreover, as C_m measurements cannot distinguish between the fusion of large dense-core granules or microvesicles, nor distinguish between the temporally overlapping processes of exocytosis and endocytosis, these measurements may underestimate the secretory capacity of individual SON neurones.

Voltage and Ca^{2+} dependence of evoked ΔC_m

Perfusion of SON neurones with the Ca^{2+} channel blocker, Cd^{2+} (100 μM), abolished the depolarization-evoked I_{Ca} and any associated ΔC_m (Fig. 1*B*). This result indicated that C_m responses were largely dependent upon depolarization-induced influx of Ca^{2+} through voltage-dependent Ca^{2+} channels. Likewise, the ΔC_m responses evoked by depolarizing pulses were abolished when the normal extracellular solution bathing the neurone was replaced with one containing no added Ca^{2+} ($n = 3$). To further assess the dependence of ΔC_m on Ca^{2+} influx, we determined the amplitude–voltage relationship for ΔC_m by evoking a series of I_{Ca} and ΔC_m responses to single 200 ms depolarizing steps in increments of 10 mV from a V_h of −90 mV. In conjunction with these recordings, ratiometric monitoring was performed of the corresponding changes in $[Ca^{2+}]_i$ in neurones that had been preloaded with the calcium-sensitive indicator, Fura-2. Figure 2*A* and *B* illustrates the results from a representative experiment.

In this neurone, ΔC_m was elicited at test potentials that evoked appreciable inward current and corresponding increases in $[Ca^{2+}]_i$ and attained maximal amplitude at +10 mV, where I_{Ca} and $[Ca^{2+}]_i$ also peaked. Conversely the evoked ΔC_m decreased as the test potential approached the estimated value for E_{Ca} (∼+70 mV), consistent with the diminishment of Ca^{2+} influx. To test whether ΔC_m might depend more directly on the total Ca^{2+} influx rather than peak I_{Ca}, we next determined the charge density of Ca^{2+} ion movement (Q_{Ca}) that resulted from a 200 ms step to a particular test potential, calculated by integrating with respect to time the area under the corresponding I_{Ca}. Figure 2*C* provides a graphic comparison of the voltage-dependence of Q_{Ca} (■) and the amplitude–voltage relationship of the corresponding ΔC_m response (▲), obtained by averaging measurements from six neurones. Although inducement of ΔC_m occurred at a higher voltage threshold than Ca^{2+} influx (−10 and −20 mV, respectively), overall the voltage relationship of ΔC_m closely followed the bell-shaped voltage profile for Q_{Ca}. Moreover, simultaneous monitoring of changes in $[Ca^{2+}]_i$ with Fura-2 showed that the depolarization-evoked increases in Q_{Ca} resulted in corresponding changes in global $[Ca^{2+}]_i$. Increases in $[Ca^{2+}]_i$ evoked by steps generated inward I_{Ca} that rose rapidly to peak values within 500 ms of the voltage pulse, after which $[Ca^{2+}]_i$ gradually returned to resting levels over tens of seconds (Fig. 2*B*). The lag in inducement of ΔC_m compared to Q_{Ca} indicated that Ca^{2+} ions entering the cell must overcome some threshold value for activation of Ca^{2+}-dependent secretion, which under our experimental conditions represented a mean influx of 37.6 pC. Because our $[Ca^{2+}]_i$ measurements report global changes in intracellular Ca^{2+}, we cannot deduce the nature of the Ca^{2+} signal that triggers exocytosis in SON neurones. Nonetheless, an additional observation offers at least some initial insight regarding its identity.

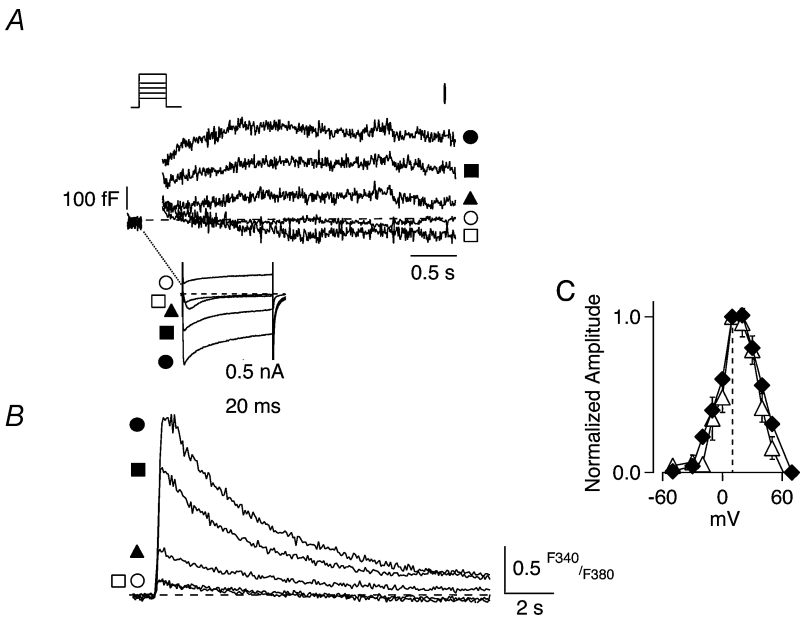

Figure 2. Voltage dependence of ΔC_m parallels that for depolarization-evoked Ca^{2+} influx
A, the relationships for I_{Ca} and ΔC_m as a function of membrane potential were determined, as shown for a representative SON neurone, by delivering a series of 200 ms depolarizing steps to different test potentials in 10 mV increments from $V_h = -90$ mV. For purposes of clarity, only selected current (lower panel) and C_m traces (upper panel) from several test potentials are shown (□, −50; ▲, −30; ●, +10; ■, +30; and ○, +70 mV). The amplitude of I_{Ca} (lower traces) increased in a voltage-dependent manner with increasing membrane depolarization up to a maximum obtained at +10 mV. A similar voltage-dependent profile was obtained for the corresponding increase in ΔC_m (upper traces) measured at the termination of each depolarizing step. *B*, the increases in I_{Ca} and ΔC_m recorded at a given test potential were accompanied by corresponding elevations in intracellular Ca^{2+} concentration ($[Ca^{2+}]_i$), as measured fluorometrically by inclusion of the Ca^{2+}-sensitive dye fura-2 in the recording pipette. Note that stepping to test potentials that evoked either negligible or outward I_{Ca} (−50 and +70 mV, respectively), resulted in little change in $[Ca^{2+}]_i$ and did not evoke ΔC_m responses. *C*, direct comparison of the complete voltage-dependent relationship for the normalized amplitude of the depolarization-evoked ΔC_m (Δ) and for the corresponding Ca^{2+} charge integral, Q_{Ca} as a function of test potential (⧫) revealed that they were tightly correlated.

In comparison to results obtained with standard internal solution (0.25 mM EGTA), our ability to evoke a ΔC_m in response to a single 200 ms depolarizing pulse to +10 mV was markedly reduced (absent in 3 of 4 neurones tested) when recordings were obtained with high EGTA (10 mM) in the recording pipette (results not shown).

Estimations of the size of the releasable vesicle pool and rate of somatic secretion

The above results underscore the similarity of the Ca^{2+}-dependent exocytotic ΔC_m responses observed for both MNC somata and MNC nerve endings (Giovannucci & Stuenkel, 1997). To further investigate this similarity we estimated the initial rate of somatic release using a series of step depolarizations of increasing duration to deplete the soma of the readily available pool of granules, using a protocol employed previously for MNC terminals (Giovannucci & Stuenkel, 1997). The traces in Fig. 3*A* illustrate the results from a representative experiment in which we compared how the evoked I_{Ca}, corresponding elevation in $[Ca^{2+}]_i$ and associated ΔC_m changed as a function of test potential duration. An increase in C_m was first detected at a pulse duration of 20 ms, and the amplitude of ΔC_m became larger as the pulse duration was lengthened up to 200 ms. Likewise, the magnitude of the induced elevation of $[Ca^{2+}]_i$ also correlated with pulse duration. Figure 3*B* summarizes the results from 10 similar experiments, showing the mean ΔC_m responses measured for each duration of the depolarizing pulse examined. The continuous line represents the best linear fit of the data, providing an exocytotic rate of 1110 fF s^{-1}, or 1533 vesicles s^{-1}. It should be appreciated, however, that these estimations might somewhat underestimate the rate of exocytosis owing to overlap of depolarizing pulses of long duration with the initial phase of the evoked ΔC_m.

Properties of the delayed C_m increase in SON neurones

In 3 of 40 neurones stimulated with single depolarization steps and in 6 of 11 neurones tested with trains of stimulations, the Ca^{2+}-dependent C_m response included an additional slowly increasing phase that emerged at variable latency after induction of the fast ΔC_m and persisted following completion of the underlying I_{Ca}. As a result, the depolarization-evoked ΔC_m in these neurones was at least biphasic, with one or more inflections in the rising phase of the C_m trace (see Fig. 1*A*, cells 2 and 3). The delayed C_m responses, which we term the secondary secretory phase ($\Delta C_{m,s}$), were only observed when neurones received single depolarizations 200 ms or longer in duration or after a repetitive series of eight to 12 pulses (50–200 ms) to test potentials that evoked maximal I_{Ca}. The latency to onset, rate of rise and amplitude of the $\Delta C_{m,s}$ varied between neurones. Typically the $\Delta C_{m,s}$ began to rise 0.5–1 s after the onset of depolarization and reached a mean maximum amplitude of 225 ± 92 fF.

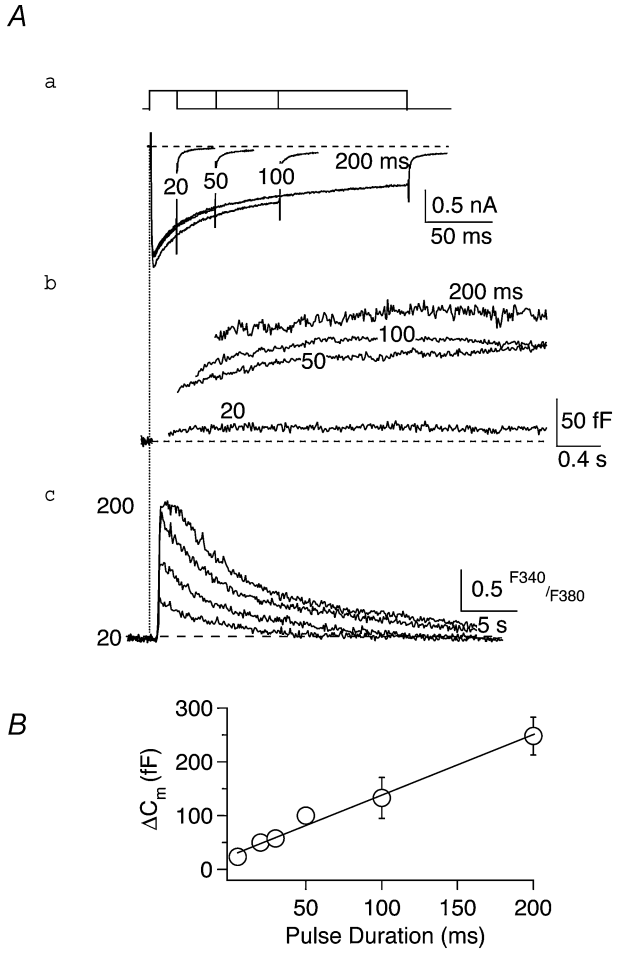

Figure 3. Determination of the rate of exocytosis
A, records from a single SON neurone illustrate the changes in I_{Ca} (*a*), ΔC_m (*b*) and $[Ca^{2+}]_i$ (*c*) evoked in response to step depolarization to +10 mV from $V_h = -90$ mV, as a function of increasing the duration of the test pulse. Increasing the duration of the depolarizing step in roughly a 2-fold manner from 20 to 200 ms resulted in a concomitant lengthening in time course of the evoked I_{Ca} (*Aa*) and progressive increases in the peak amplitude of the corresponding ΔC_m (*Ab*). *Ac*, the progressive increases in duration of the evoked Ca^{2+} influx and in peak ΔC_m were paralleled by corresponding higher accumulations in $[Ca^{2+}]_i$. *B*, plotting of the averaged ΔC_m evoked by depolarization +10 mV from $V_h = -90$ mV in 5 neurones, as a function of test pulse duration, yielded a linear relationship that could be best described by the following function (straight line): $\Delta C_m = 1.11 \times$ (pulse duration) + 27.2. The slope of this relationship indicates the initial rate of secretion was 1110 fF s^{-1}, or 1533 vesicles s^{-1}, under the present experimental conditions.

It is worth noting that in MNC nerve endings, a similar, latent and slowly rising Ca^{2+}-dependent C_m increase can be evoked in response to prolonged or repetitive step depolarizations (Seward *et al.* 1995; Giovannucci & Stuenkel, 1997). In this preparation, such responses required higher elevation in $[Ca^{2+}]_i$ for activation, compared to the initial ΔC_m and have been attributed, based on their additional properties (e.g. sensitivity to Ca^{2+} diffusion and exogenous buffering), to secretion from a distinct releasable granule pool (RRP) of larger capacity (Seward *et al.* 1995; Giovannucci & Stuenkel, 1997). The requirement of a larger Ca^{2+} influx to evoke the $\Delta C_{m,s}$ was also found after normalizing the Q_{Ca} for resting whole-cell C_m, arguing against the possibility that this might be related simply to differences in cell size. The protocols required to generate the $\Delta C_{m,s}$ resulted in marked inter-trial variability and rapid rundown in the evoked ΔC_m, precluding a more vigorous analysis of this latent and more sustained secretory response. Nevertheless, the above results strongly suggest that a $\Delta C_{m,s}$ was only induced after the cumulative number of Ca^{2+} ions entering the cell overcame a threshold whose value exceeded that required for activation of secretion from an immediately releasable pool. In addition, they are consistent with the hypothesis that somatic secretion in SON neurones may involve the recruitment and Ca^{2+}-dependent exocytosis of granules from more than one vesicular pool, recapitulating at least to some degree the events associated with depolarization-evoked release from their neurosecretory nerve endings.

Activation of I_{Ca} with action potential waveforms

The pulsatile stimuli used initially to examine for exocytotic activity in SON neurones generated Ca^{2+} currents unlikely to be encountered during normal spike behaviour. Therefore, an additional series of experiments was performed to ascertain whether somatic secretion could be supported by Ca^{2+} signals that more closely conform to those associated with physiological patterns of SON neuronal activity. For these experiments, we first recorded an action potential from a SON neurone under current clamp and reconstructed the action potential waveform (APW) for use as a voltage-clamp stimulus template to evoke action potential-generated currents. The APW depicted in Fig. 4*A* (upper trace) began from a baseline holding potential of −60 mV, and included an initial slow 2 ms voltage ramp to approximately −40 mV, followed by a rapid overshoot to approximately 20 mV and a subsequent rapid recovery back toward baseline, terminating with a slower afterhyperpolarization to −83 mV. The action potential properties depicted by this APW are similar to those previously characterized for SON neurone action potential firing recorded *in vivo* (Armstrong *et al.* 1994) and in slice preparations (Jourdain *et al.* 1998). A negative-directed APW (nAPW) of identical morphology, but opposite polarity, was also constructed and used as a voltage-clamp template to measure leak

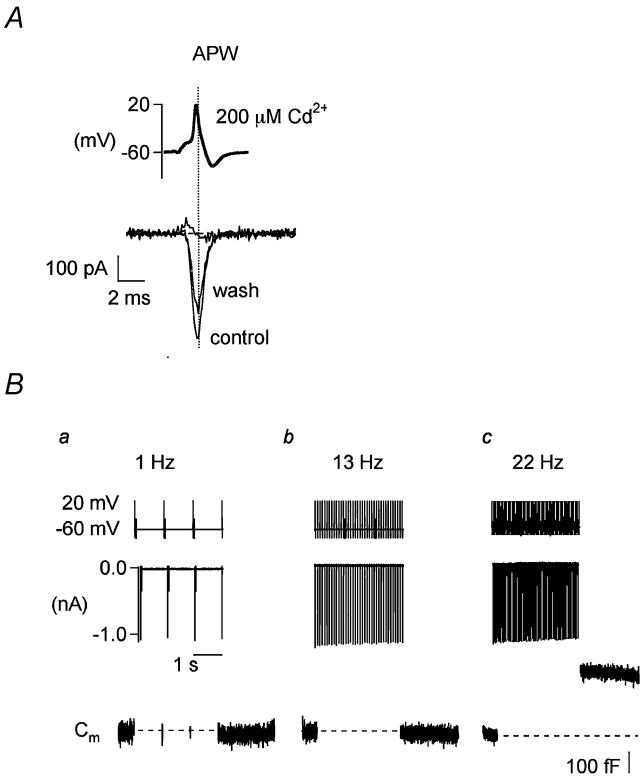

Figure 4. APWs generate frequency-dependent C_m responses in SON neurones

A, the top trace depicts an APW voltage template (upper trace) that was constructed from a spontaneous action potential recorded under current clamp conditions in an acutely isolated SON neurone. Presentation of this APW as a stimulus template under voltage clamp evoked a large inward current in a representative SON neurone (lower traces, control). The evoked current was reversibly blocked by administration of the Ca^{2+} channel blocker Cd^{2+} (200 μM, asterick). *B*, I_{Ca} (middle traces) and ΔC_m (lower traces) evoked by presentations of APW stimuli in another neurone are shown on a compressed time scale, as compared to that in *A*, such that APWs (top traces) and I_{Ca} (middle traces) appear as single lines above or below baseline, respectively. Baseline C_m measurements were obtained at $V_h = -60$ mV (lower traces) before delivery of a train of APWs at frequencies of 1 Hz (*Ba*), 13 Hz (*Bb*) and 22 Hz (*Bc*). The detection period for monitoring changes in capacitance in response APW presentations comprised a 15 ms window at the end of the second delivery of APW stimuli over a total 3 s stimulation time period, after which continual capacitance detection was performed for another 3 s (lower traces). Middle traces illustrate the evoked I_{Ca} responses corresponding to each presentation of APW at the indicated frequency.

current (not shown). The nAPW-generated leak current traces were subtracted from uncorrected APW-generated current traces to obtain a measure of the APW-evoked inward currents. Under the same recording conditions used above to study step-evoked HVA Ca^{2+} currents, the APW-generated inward current response activated with peak depolarization of the APW, suggesting that this current required strongly depolarized potentials (>0 mV) for activation. The peak of the current response occurred during the falling phase of the APW (dotted line, Fig. 4). In addition, the current was reversibly blocked by Cd^{2+} treatment (200 μM; Fig. 4*A*, lower traces). This indicated that Ca^{2+} influx was through voltage-activated Ca^{2+} channels. We have previously shown that these APW-generated Ca^{2+} currents reflect the activation of L-, N-, R- and P/Q-type Ca^{2+} channels (Soldo *et al.* 1998).

APW-generated secretory responses

In the following experiments, individual SON neurones were clamped to $V_h = -60$ mV and baseline C_m was measured, after which APWs were delivered as the depolarizing stimulus. The APW-evoked current responses were recorded during a train of APWs. C_m measurements were captured in a 15 ms window and obtained at 1 Hz throughout the duration of the train (Fig. 4*B*). We applied APWs at physiologically relevant frequencies. Measurements of C_m (lower traces) obtained following presentation of each APW during a 3 s train of stimuli applied at a frequency of 1 Hz showed no change from baseline, as illustrated in Fig. 4*Ba*. Likewise, a 3 s train of APWs applied at frequencies up to 13 Hz (see Fig. 4*Bb*) was ineffective in eliciting an increase in C_m. On the other hand, trains of APWs delivered at these frequencies induced substantial I_{Ca} (Fig. 4*B*, middle traces). In contrast, a robust ΔC_m was reliably evoked when APWs were presented at frequencies of 22 Hz or higher. For example, as shown in Fig. 4*Bc*, a robust ΔC_m response was elicited within 2 s following application of a 22 Hz stimulus. Interestingly, unlike step depolarizations, APWs did not elicit the ΔC_t. Neither nAPW nor trains of APW during Cd^{2+} blockade of Ca^{2+} influx induced a change in C_m. Thus no subtraction protocol for these records was performed.

Milk ejection-like burst pattern of APWs maintains secretion

OT- and aVP-containing SON neurones have been shown to exhibit specific patterns of action potential bursting that can be correlated with particular types of physiological stimuli, including suckling and parturition. For example, during the milk ejection reflex that occurs with suckling, OT neurones demonstrate a specific bursting pattern of discharge (ME burst) that is believed to sustain secretion of OT that, in turn, supports milk production. The ME burst pattern, characterized by *in vivo* recordings from rats (Jourdain *et al.* 1998), consists of a baseline discharge of low AP firing frequency (~6 Hz) which, upon the burst, quickly reaches a peak frequency of firing of ~33 Hz and then declines at a slower rate back to baseline (see Jourdain *et al.* 1998 – Fig. 4*B*1). In a final series of experiments, we closely modelled this ME burst pattern with trains of APWs (Fig. 5*A*) and used this as a stimulus template to examine its ability to support exocytotic release from SON somata. When applied as the depolarizing stimulus, each APW in the ME burst template activated a brief inward current, as illustrated in Fig. 5*B*. The Ca^{2+} currents evoked by consecutive APWs of the burst stimulus are represented sequentially on the condensed time scale by the downward strokes below baseline, and these responses appeared similar in morphology and peak amplitude to those already described. The corresponding ΔC_m response elicited by the ME burst of APWs is depicted in Fig. 5*D* (trace *a*). The initial 1 s presentation of APWs at the baseline rate of 6 Hz did not elicit a ΔC_m. By contrast, the subsequent delivery of higher frequency trains of APWs, first at 33 Hz, followed by gradual changes in frequency to 11 Hz resulted in substantial increases in ΔC_m. Measurements taken 1 s after initiation of the 33 Hz train of APWs revealed a robust ΔC_m with incremental increases in C_m registered after delivery of each successive 1 s train of APWs throughout the duration of the ME burst pattern. Interestingly, the ΔC_m continued to increase even as the frequency of APW presentation in the template declined below 22 Hz, a level estimated previously to represent the threshold for activation of a secretory response in these neurones (see Fig. 4*B*). In fact, upon cessation of the ME burst, the C_m trace displayed a slow, continual increase for a number of seconds thereafter. This latter result is entirely consistent with an increasing elevation in global $[Ca^{2+}]_i$ to a level capable of sustaining secretory responses. Presentation of an ME burst of 'negative' APWs (nAWPs) resulted in small inward leak currents (Fig. 5*C*), but failed to elicit a C_m response in this neurone (Fig. 5*D*, trace*b*). Results similar to these were observed in three additional neurones examined in this manner.

Although we did not consistently identify OT neurones in this study, in some experiments we identified single soma-type postrecording using aVP- or OT-specific antisera (dot blot method previously described in Soldo & Moises, 1998). In 16 cases we were able to conclusively

identify neurone type (roughly 50 : 50 distribution, one neurone expressing both aVP and OT). No consistent difference in the C_m responses between the two cell types was observed. This indicates that the Ca^{2+}-dependent C_m increases can be induced in both OT and aVP soma and that stimulus pattern or frequency may be a major determinant of electrical activity-induced release characteristics.

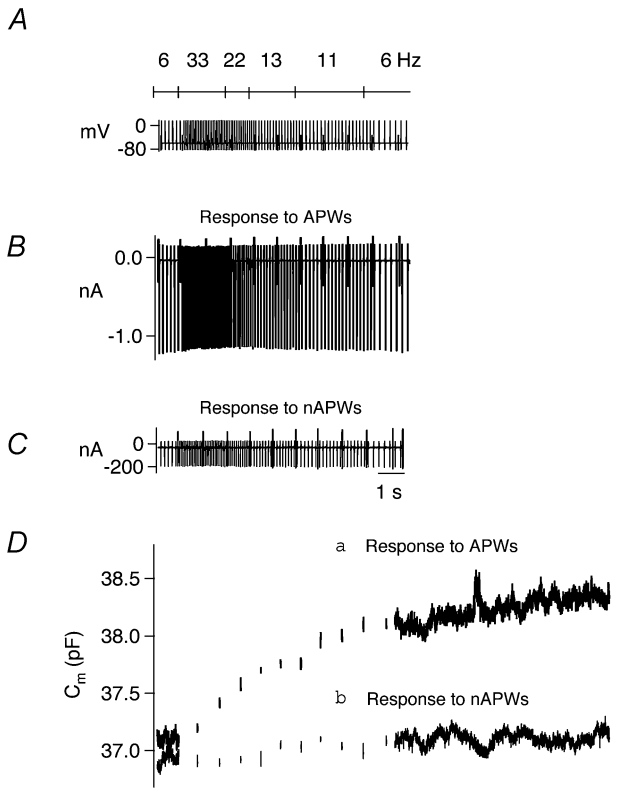

Figure 5. I_{Ca} and corresponding ΔC_m responses evoked by presentation of a physiologically relevant APW voltage template

A, lower trace illustrates the composition of an APW voltage template modelled after an OT burst of action potentials during the milk ejection reflex (see Jourdain *et al.* 1998; Fig. 4*B*1). The OT-patterned APW burst was comprised of multiple 1 s segments, apportioned into successive trains of individual APW at frequencies of 6, 33, 33, 22, 13, 13, 11, 11, 11 and 6 Hz. *B*, continuous recording of individual I_{Ca} responses evoked in response to the OT-like train of APWs. Note the small decrement in peak amplitude of I_{Ca} evoked at the higher frequency APW trains (33 and 22 Hz), and restoration of peak amplitudes that occurs with delivery of the subsequent lower frequency trains. *C*, leak current responses evoked by deliverying a burst of negative APWs applied at the same frequencies as the OT-patterned burst of APWs. *D*, baseline capacitance measurements were obtained for several seconds before presentation of the OT-patterned APW burst. Subsequent to initiation of the burst, C_m measurements were obtained once every second within a 15 ms window (trace*a*). C_m measurements were also obtained during a similar train of nAPWs (trace *b*). Note that increases in ΔC_m were first evoked during the 33 Hz APW trains, and then either continued to increase or reached a plateau with presentations of APW trains at lower frequency.

Discussion

There is a growing consensus that the neuropeptide OT regulates rhythmic electrical activity and development of MNCs at the level of the SON. It has been proposed that MNCs may independently regulate the pulsatile release of OT via positive retrograde signalling (Moos *et al.* 1984; Jourdain *et al.* 1998) and the inhibition of excitatory afferents (Hirasawa *et al.* 2001; Kombian *et al.* 2002). In addition, OT signalling has been proposed to induce morphological and developmental changes in MNCs (Chevaleyre *et al.* 2000, 2001).

In this paper we used time-resolved membrane capacitance measurements to directly demonstrate that isolated MNC somata undergo Ca^{2+}-dependent secretory activity. Importantly, our work reveals that the neuronal somata exhibit multiple phases of C_m, indicating that there are functionally distinct secretory granule pools, similar to that observed in their isolated nerve terminals (Lim *et al.* 1990; Seward *et al.* 1995; Hsu & Jackson, 1996; Giovannucci & Stuenkel, 1997; Nowycky *et al.* 1998). The Ca^{2+} and activity dependence of these phases indicate that functional exocytotic machinery is also present in the somata and that Ca^{2+}-dependent exocytotic activity underlies somatodendritic peptidergic secretion. Thus, modulation of the sizes of these granule pools might provide a basis for plasticity of the secretory response to meet specific physiological demands.

C_m detection in conjunction with whole-cell voltage clamp revealed that exocytotic events were preferentially evoked with depolarizing voltage steps or with high frequency action potential waveform stimulations that evoked substantial Ca^{2+} influx via activation of voltage-gated Ca^{2+} channels. Voltage-dependent capacitance responses consisted of at least three phases: (1) an initial Ca^{2+}-independent transient component that obfuscated the first 10–15 ms of the Ca^{2+}-dependent C_m components; (2) a residual Ca^{2+}-dependent ΔC_m that could be measured following subtraction of the Ca^{2+}-independent transient and cessation of the depolarizing voltage pulse; and (3) a more persistent component that induced ΔC_m with varying delays. Accordingly, we have termed the two Ca^{2+}-dependent C_m components as indicative of rapidly releasable and slowly releasable secretory granule pools, respectively.

The Ca^{2+} dependence of the ΔC_m attributed to the rapidly releasable pool was established by abolition of the evoked ΔC_m during Ca^{2+} channel blockade, by showing a

correlation between the voltage–response relationship of Ca^{2+} channel activation and ΔC_m, and by demonstrating linearity between the flux of Ca^{2+} across the membrane and peak ΔC_m amplitudes. It has been previously shown in neurohypophysial nerve endings that Ca^{2+}-dependent increases in C_m eventually saturate and that this property may reflect the release from, and the eventual depletion of, a rapidly releasable pool of vesicles that are primed and docked at the cellular membrane (Giovannucci & Stuenkel, 1997). The C_m increase detected immediately following a brief depolarization was interpreted to reflect the exocytosis of a subpopulation of vesicles that are immediately available to fuse with the membrane. Likewise, stepwise changes in C_m were evoked in MNC somata in response to brief depolarizations, and these changes eventually saturated when challenged by repetitive stimulations. The diminution of the ΔC_m occurred despite evidence that $[Ca^{2+}]_i$ continued to increase beyond this point. This observation is consistent with the depletion of an immediately releasable pool of granules that is sensitive to localized domains of high Ca^{2+} influx. In several neurones we detected a delayed and persistent ΔC_m that was initiated during repetitive pulses or that appeared to activate several seconds beyond termination of long-duration pulses. Because of the variability of the delayed ΔC_m, and the small number of cells that exhibited this profile, we did not investigate these events further. However, similar responses have been described in neurohypophysial nerve endings and chromaffin cells and postulated to reflect the recruitment of a slowly releasable pool of vesicles.

Although we clearly demonstrated that step depolarizations applied either repetitively or with long duration could evoke secretory activity, we also tested whether such activity could be induced using stimulations and experimental conditions that were more physiologically relevant. An additional set of experiments demonstrated that action potential waveforms, capable of activating short duration inward I_{Ca}, could evoke ΔC_m in SON neurones if applied in trains of greater than 22 Hz. The Ca^{2+} efficacy of trains of high-frequency APW stimulations to evoke exocytotic responses may be greater than that of depolarizing pulses due to a relationship between Ca^{2+} entry and the interpulse interval between stimulations (Engisch *et al.* 1997). That intermittent stimulations can maintain increases in ΔC_m suggests that the secretory machinery is capable of summating small quantities of Ca^{2+} entry per APW stimulation. Moreover, the repetitive stimulus protocol used here spans several seconds, which provides sufficient time for activation of Ca^{2+}-dependent signalling systems. In addition, recent evidence suggests that Ca^{2+}-induced Ca^{2+} release or OT or AVP evoked Ca^{2+} release from internal Ca^{2+} stores might play a role in modulating the release of peptide from the cell bodies of MNCs.

Our results support previous findings that have indicated exocytotic activity at extrasynaptic sites. Ultrastructural data have provided indirect evidence that is consistent with the exocytosis of vesicles at both synaptic and non-synaptic somatodendritic sites (sympathetic ganglia: Zaidi & Matthews, 1997; supraoptic nucleus: Pow & Morris, 1989; Wang *et al.* 1995). Direct measurements obtained using amperometry and single-cell immunoblots have provided strong evidence for Ca^{2+}-dependent secretion of monoamines and neuropeptides from cell bodies in central and spinal cord neurones (substantia nigra: (Cheramy *et al.* 1981; Jaffe *et al.* 1998; dorsal root ganglia: Huang & Neher, 1996).

The C_m measurements of suproptic neurones described in the current study and one previously reported (Soldo *et al.* 1998) indicate that electrical activity at the cell soma can induce Ca^{2+}-dependent exocytotic activity. These data largely agree with C_m measurements of supraoptic neurones recently reported by de Kock *et al.* (2003). However, whereas de Kock *et al.* observed C_m changes induced by application of a single AP waveform, a major observation of our study was that repetitive application of AP waveforms was required to evoke C_m increases. Application of a single AP waveform under our conditions induced only a Ca^{2+}-independent C_m transient, consistent with our previous demonstration that a short-duration depolarization (<5 ms) in isolated neurohypophysial nerve terminals was ineffective at consistently evoking an exocytotic response. The observation that robust, prolonged electrical activity that induced substantial rises in $[Ca^{2+}]_i$ was required to induce somatic C_m increases indicates that dendritic release of peptide may be highly regulated. Thus, although our work and the work of others (Kombian *et al.* 1997; De Kock *et al.* 2003) clearly indicates that Ca^{2+} influx through voltage-dependent Ca^{2+} channels can induce the release of neuropeptide, it does not suggest that influx is necessarily the preferred route by which OT is released from dendrites. In fact work of Ludwig *et al.* (2002) demonstrated that increases in dendritic $[Ca^{2+}]_i$ activates and enhances OT release, whereas back propagation of AP from the neural stalk was ineffective. As such, the apparent differences in the control of peptide release reported in these studies may indicate modulation of size of the releasable pool of secretory vesicles and the plastic nature of somatodendritic secretion.

Thus, our work supports and extends the concept of somatodendritic release as an important regulator of

hypothalamic rhythmicity and development, and indicates that exocytotic release of peptide from somata or dendrites participates in a bidirectional pathway for communication between pre- and postsynaptic elements within the SON.

References

Armstrong WE, Smith BN & Tian M (1994). Electrophysiological characteristics of immunochemically identified rat oxytocin and vasopressin neurones *in vitro*. *J Physiol* **475**, 115–128.

Bezanilla F, Taylor RE & Fernandez JM (1982). Distribution and kinetics of membrane dielectric polarization. 1. Long-term inactivation of gating currents. *J General Physiol* **79**, 21–40.

Cheramy A, Leviel V & Glowinski J (1981). Dendritic release of dopamine in the substantia nigra. *Nature* **289**, 537–542.

Chevaleyre V, Dayanithi G, Moos FC & Desarmenien MG (2000). Developmental regulation of a local positive autocontrol of supraoptic neurons. *J Neurosci* **20**, 5813–5819.

Chevaleyre V, Moos FC & Desarmenien MG (2001). Correlation between electrophysiological and morphological characteristics during maturation of rat supraoptic neurons. *Eur J Neurosci* **13**, 1136–1146.

De Kock CP, Wierda KD, Bosman LW, Min R, Koksma JJ, Mansvelder HD, Verhage M & Brussaard AB (2003). Somatodendritic secretion in oxytocin neurons is upregulated during the female reproductive cycle. *J Neurosci* **23**, 2726–2734.

Debus K, Hartmann J, Kilic G & Lindau M (1995). Influence of conductance changes on patch clamp capacitance measurements using a lock-in amplifier and limitations of the phase tracking technique. *Biophys J* **69**, 2808–2822.

Di Scala-Guenot D, Strosser MT & Richard P (1987). Electrical stimulations of perifused magnocellular nuclei *in vitro* elicit Ca^{2+}-dependent, tetrodotoxin-insensitive release of oxytocin and vasopressin. *Neurosci Lett* **76**, 209–214.

Engisch KL, Chernevskaya NI & Nowycky MC (1997). Short-term changes in the Ca^{2+}-exocytosis relationship during repetitive pulse protocols in bovine adrenal chromaffin cells. *J Neurosci* **17**, 9010–9025.

Fisher TE & Bourque CW (1995). Voltage-gated calcium currents in the magnocellular neurosecretory cells of the rat supraoptic nucleus. *J Physiol* **486**, 571–580.

Foehring RC & Armstrong WE (1996). Pharmacological dissection of high-voltage-activated Ca^{2+} current types in acutely dissociated rat supraoptic magnocellular neurons. *J Neurophysiol* **76**, 977–983.

Gentet LJ, Stuart GJ & Clements JD (2000). Direct measurement of specific membrane capacitance in neurons. *Biophys J* **79**, 314–320.

Giovannucci DR & Stuenkel EL (1997). Regulation of secretory granule recruitment and exocytosis at rat neurohypophysial nerve endings. *J Physiol* **498**, 735–751.

Hamill OP, Marty A, Neher E, Sakmann B & Sigworth FJ (1981). Improved patch-clamp techniques for high-resolution current recording from cells and cell-free membrane patches. *Pflugers Arch* **391**, 85–100.

Hirasawa M, Kombian SB & Pittman QJ (2001). Oxytocin retrogradely inhibits evoked, but not miniature, EPSCs in the rat supraoptic nucleus: role of N- and P/Q-type calcium channels. *J Physiol* **532**, 595–607.

Horrigan FT & Bookman RJ (1994). Releasable pools and the kinetics of exocytosis in adrenal chromaffin cells. *Neuron* **13**, 1119–1129.

Hsu SF & Jackson MB (1996). Rapid exocytosis and endocytosis in nerve terminals of the rat posterior pituitary. *J Physiol* **494**, 539–553.

Huang LY & Neher E (1996). Ca^{2+}-dependent exocytosis in the somata of dorsal root ganglion neurons. *Neuron* **17**, 135–145.

Jaffe EH, Marty A, Schulte A & Chow RH (1998). Extrasynaptic vesicular transmitter release from the somata of substantia nigra neurons in rat midbrain slices. *J Neurosci* **18**, 3548–3553.

Joshi C & Fernandez JM (1988). Capacitance measurements. An analysis of the phase detector technique used to study exocytosis and endocytosis. *Biophys J* **53**, 885–892.

Jourdain P, Israel JM, Dupouy B, Oliet SH, Allard M, Vitiello S, Theodosis DT & Poulain DA (1998). Evidence for a hypothalamic oxytocin-sensitive pattern-generating network governing oxytocin neurons *in vitro*. *J Neurosci* **18**, 6641–6649.

Kombian SB, Hirasawa M, Mouginot D & Pittman QJ (2002). Modulation of synaptic transmission by oxytocin and vasopressin in the supraoptic nucleus. *Prog Brain Res* **139**, 235–246.

Kombian SB, Mouginot D & Pittman QJ (1997). Dendritically released peptides act as retrograde modulators of afferent excitation in the supraoptic nucleus *in vitro*. *Neuron* **19**, 903–912.

Lambert RC, Moos FC & Richard P (1993). Action of endogenous oxytocin within the paraventricular or supraoptic nuclei: a powerful link in the regulation of the bursting pattern of oxytocin neurons during the milk-ejection reflex in rats. *Neuroscience* **57**, 1027–1038.

Lim NF, Nowycky MC & Bookman RJ (1990). Direct measurement of exocytosis and calcium currents in single vertebrate nerve terminals. *Nature* **344**, 449–451.

Lindau M & Neher E (1988). Patch-clamp techniques for time-resolved capacitance measurements in single cells. *Pflugers Arch* **411**, 137–146.

Ludwig M, Sabatier N, Bull PM, Landgraf R, Dayanithi G & Leng G (2002). Intracellular calcium stores regulate activity-dependent neuropeptide release from dendrites. *Nature* **418**, 85–89.

Mason WT, Ho YW & Hatton GI (1984). Axon collaterals of supraoptic neurones: anatomical and electrophysiological evidence for their existence in the lateral hypothalamus. *Neuroscience* **11**, 169–182.

Moos F, Freund-Mercier MJ, Guerne Y, Guerne JM, Stoeckel ME & Richard P (1984). Release of oxytocin and vasopressin by magnocellular nuclei *in vitro*: specific facilitatory effect of oxytocin on its own release. *J Endocrinol* **102**, 63–72.

Moos F, Poulain DA, Rodriguez F, Guerne Y, Vincent JD & Richard P (1989). Release of oxytocin within the supraoptic nucleus during the milk ejection reflex in rats. *Exp Brain Res* **76**, 593–602.

Neher E & Marty A (1982). Discrete changes of cell membrane capacitance observed under conditions of enhanced secretion in bovine adrenal chromaffin cells. *Proc Natl Acad Sci U S A* **79**, 6712–6716.

Neumann I, Ludwig M, Engelmann M, Pittman QJ & Landgraf R (1993). Simultaneous microdialysis in blood and brain: oxytocin and vasopressin release in response to central and peripheral osmotic stimulation and suckling in the rat. *Neuroendocrinology* **58**, 637–645.

Nowycky MC, Seward EP & Chernevskaya NI (1998). Excitation-secretion coupling in mammalian neurohypophysial nerve terminals. *Cell Mol Neurobiol* **18**, 65–80.

Pow DV & Morris JF (1989). Dendrites of hypothalamic magnocellular neurons release neurohypophysial peptides by exocytosis. *Neuroscience* **32**, 435–439.

Seward EP, Chernevskaya NI & Nowycky MC (1995). Exocytosis in peptidergic nerve terminals exhibits two calcium-sensitive phases during pulsatile calcium entry. *J Neurosci* **15**, 3390–3399.

Soldo BL, Giovannucci DR, Stuenkel EL & Moises HC (1998). Opioids modulate Ca^{2+} currents evoked by action potential waveforms in rat supraoptic nucleus neurons. *J Neurosci* **24**, 1081.

Soldo BL & Moises HC (1998). μ-Opioid receptor activation inhibits N- and P-type Ca^{2+} channel currents in magnocellular neurones of the rat supraoptic nucleus. *J Physiol* **513**, 787–804.

Wang H, Ward AR & Morris JF (1995). Oestradiol acutely stimulates exocytosis of oxytocin and vasopressin from dendrites and somata of hypothalamic magnocellular neurons. *Neuroscience* **68**, 1179–1188.

Zaidi ZF & Matthews MR (1997). Exocytotic release from neuronal cell bodies, dendrites and nerve terminals in sympathetic ganglia of the rat, and its differential regulation. *Neuroscience* **80**, 861–891.

Acknowledgements

We thank Dr Xiaoming Hou and Bi Yu for providing technical assistance, and Charles Pluto for comments. Various portions of this work were supported by an American Heart Association Scientist Development Grant 0130231N to D.R.G., National Institute on Drug Abuse Grants DA 03365 to H.C.M and DA 07268 (postdoctoral training fellowship) to B.L.S, and NIH Grant NS 39914 to E.L.S.

Author's present address

B. L. Soldo: Pfizer Global R & D, 2800 Plymouth Road, Ann Arbor, MI 48105, USA.